Physics of the Earth and Planetary Interiors 177 (2009) 31–45

Contents lists available at ScienceDirect

Physics of the Earth and Planetary Interiors

journal homepage: www.elsevier.com/locate/pepi

Paleosecular variation models for ancient times: Clues from Keweenawan lava flows

Lisa Tauxe[a,*], Kenneth P. Kodama[b]

[a] *Scripps Institution of Oceanography, University of California, La Jolla, CA 92093-0220, United States*
[b] *Lehigh University, Bethlehem, PA, United States*

ARTICLE INFO

Article history:
Received 24 February 2009
Received in revised form 28 June 2009
Accepted 1 July 2009

Keywords:
Paleosecular variation models
Geomagnetic field behavior
Inclination error correction
Octupole contribution to time averaged field
Asymmetric reversal behavior

ABSTRACT

Statistical paleosecular variation models predict distributions of paleomagnetic vectors as a function of geographic position. Such models have been used in a variety of applications that test whether a given data set fairly represents the variability and average properties of the geomagnetic field. The simple relationship between inclination of the geomagnetic field and latitude predicted by geocentric axial dipole (GAD) models has been a cornerstone for plate reconstructions for decades, yet many data sets exhibit a tendency to be shallower than expected for a dominantly axial geocentric magnetic field. Too shallow inclinations have variously been interpreted as plate motion, permanent non-dipole field components or bias in inclination from sedimentary processes. Statistical PSV models could in principle be used to resolve the cause of inclination anomalies because there is a simple relationship between the elongation of the distribution of directions in the vertical plane and the average inclination. Shallowing of inclinations from sedimentary processes results in a progressive transformation of the elongation direction in the vertical plane containing the average direction into a pronounced elongation in the plane perpendicular to that. However, the applicability of statistical models based on the last 5 million years for more ancient times is an open question. Here we present new data from the Keeweenawan North Shore Volcanics (~1.1 Ga). These data are consistent with statistical PSV model predictions and are less well fit by models that include a 20% axial octupole component. We also find evidence for a pervasive overprinting by hematite in a shallower direction and find support for the contention that the asymmetric reversal(s) observed in Keweenawan aged rocks along the North shore of Lake Superior can be explained as an age progression, with the reverse directions being older than the normal directions. Finally, we re-consider implications from an analysis of inclinations from the Global Paleomagnetic Database for the Paleozoic and Pre-Cambrian. We find that the data are inconsistent with a random sampling of any simple geomagnetic field model and conclude that the data set under-samples the field in a spatial sense.

1. Introduction

Statistical paleosecular variation (PSV) models for the geomagnetic field have been developed based on directional data from lava flows erupted over the last 5 million years (e.g., Constable and Parker, 1988; Quidelleur and Courtillot, 1996; Constable and Johnson, 1999; Tauxe and Kent, 2004). These predict distributions of paleomagnetic vectors (and their transformations into virtual geomagnetic poles and dipole moments) as a function of geographic position. The simple relationship between inclination of the geomagnetic field and latitude predicted by geocentric axial dipole (GAD) models has been a cornerstone for plate reconstructions for decades, yet many data sets exhibit a tendency to be shallower than expected for a dominantly axial geocentric magnetic field. These "too shallow" inclinations have variously been interpreted as plate motion, permanent non-dipole field components or inclination error. A means of discriminating among these mechanisms is essential for resolving puzzles, such as the "snow-ball earth" hypothesis (which relies in part on shallow paleomagnetic directions in direct association with sea-level glacial deposits, e.g., Sohl et al., 1999), a greater than expected frequency of shallow directions at certain times (Kent and Smethurst, 1998) or in certain places (e.g., Chauvin et al., 1996).

Statistical PSV models could in principle be used to assess whether a given distribution of paleomagnetic directions are likely to be geomagnetic in origin as opposed to one that has been distorted by sedimentary processes. The models predict a simple relationship between the elongation of the distribution of directions in the vertical plane and the average inclination. Shallowing of inclinations from sedimentary processes, on the other

* Corresponding author. Tel.: +1 858 534 6084; fax: +1 858 534 0784.
E-mail address: ltauxe@ucsd.edu (L. Tauxe).

0031-9201/$ – see front matter © 2009 Elsevier B.V. All rights reserved.
doi:10.1016/j.pepi.2009.07.006

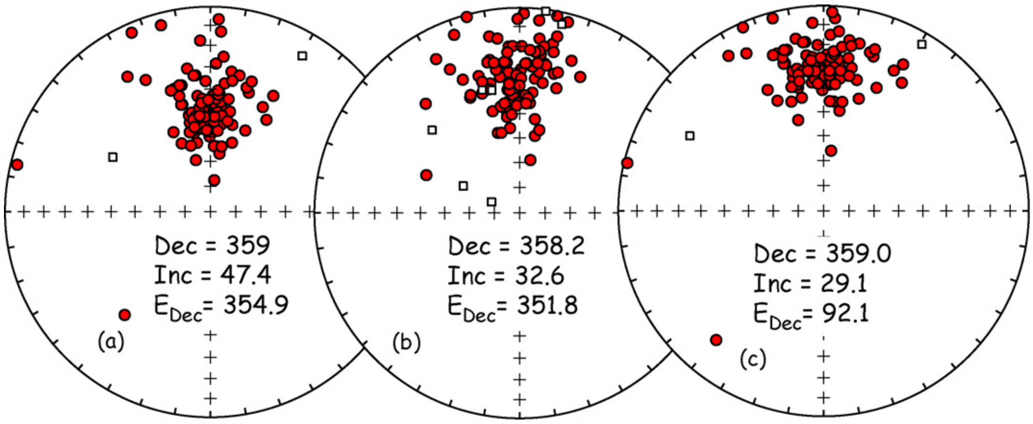

Fig. 1. (a) 100 directions drawn from the TK03.GAD field model (Tauxe and Kent, 2004; Tauxe et al., 2008) assuming a latitude of 30°N. Circles are lower hemisphere and squares are upper hemisphere. Note that the elongation direction (E_{Dec}) is parallel to the mean direction (*Dec*). (b) 100 directions drawn from the TK03.g30 model (average octupole was 20% of the dipole). (c) Directions from (a) subjected to the inclination shallowing formula with $f = 0.5$ (see text). Note that the elongation direction (E_{Dec}) is perpendicular to the mean direction (*Dec*).

hand transforms this vertical plane elongation progressively into a pronounced horizontal elongation during which the elongation direction E_{Dec} rotates from being parallel to the average direction and in the vertical plane to being perpendicular to that plane. Tauxe and Kent (2004) suggested that remanence directions could be "unflattened" using the empirical formula of (e.g., King, 1955) until the elongation and inclination agrees with the model prediction. In Fig. 1a, we show 100 directions drawn from the TK03.GAD model of Tauxe and Kent (2004) (see also Tauxe et al., 2008) for a latitude of 30°. The mean inclination is 47°, quite close to the GAD expectation of 49°. The scatter in equivalent VGPs (S_p calculated with the cut-off procedure Vandamme and Courtillot, 1992, as in McElhinny and McFadden, 1997) is 12.5^{14}_{11}. This is consistent with the prediction of 14° from Model G of McElhinny and McFadden (1997) which was tuned to the same data set as TK03.GAD. The distribution of directions is somewhat elongate ($E\sim$ 1.8 as defined by Tauxe and Kent, 2004), with the elongation direction (E_{Dec}) in the vertical plane parallel to the average direction. In fact, TK03.GAD and similar models (e.g., CJ98 of Constable and Johnson, 1999, and QC96 of Quidelleur and Courtillot, 1996) predict that elongation varies inversely with inclination. Moreover, Tauxe et al. (2008) showed that the elongation/inclination trend is fairly robustly determined for the last 5 million years and is not strongly dependent on the exact (GAD) field model chosen.

Interrogating the TK03 field model with a non-zero axial octupolar contribution of 20%, generates sets of directions like those shown in Fig. 1b. The mean inclination of 32.6° is much shallower than the GAD expectation and the distribution of directions is more elongate ($E\sim$3.1). Importantly however, E_{Dec} is still in the vertical plane parallel to the average direction.

On the other hand, distributions of directions that exhibit sedimentary inclination error are profoundly different than any statistical PSV model. The King function (King, 1955) for inclination shallowing transforms the inclination of the applied magnetic field (I_f) to the observed inclination (I_o) by: $\tan I_o = f \tan I_f$) where f is an empirical parameter ranging from 1.0 (no flattening) to 0.0 (complete flattening). The directions drawn from the TK03.GAD field model in Fig. 1a transform to those shown in Fig. 1c (assuming $f = 0.5$). While these directions have a shallow bias ($I = 29.1$) equivalent to that resulting from $\bar{g}_3^0$ of 20%, the elongation direction is perpendicular to the average direction, markedly different from the non-GAD predictions.

If statistical PSV models accurately predict distributions of directions for ancient times, such models can be used to discriminate between the different hypotheses for shallow inclination bias. This approach has been successfully carried out on data ranging from the Triassic to the present (e.g., Tauxe and Kent, 2004; Krijgsman and Tauxe, 2004; Kent and Tauxe, 2005; Tauxe, 2005; Tauxe et al., 2008). However, the PSV models used are based on compilations of paleomagnetic data for the last 5 million years and may not apply in ancient times (see discussion in Merrill et al., 1996). A quick test of the model predictions requires a large set of paleomagnetic data directions (~100) for which paleohorizontal is well constrained and plate motion over the time span of observation can be neglected. The elongation and average inclination of the data set can then be compared with the predicted trend.

Tauxe et al. (2008) compiled published data from large igneous provinces (LIPs) to address the issue of how far back in time the E/I predicted trend was valid. All LIP data sets had elongation/inclination pairs that were consistent with the PSV model predictions but the oldest LIP with suitable data was the Paraná magmatic province, of early Cretacous age. To test the applicability of E/I trends derived from PSV models to the Pre-Cambrian, we require a set of paleomagnetic directions that faithfully recorded the geomagnetic field vector whose paleohorizontal is well constrained. The data set must also sample a period of time sufficient to characterize PSV, but short enough to exclude the effects of plate motion (~ 5 million years). The mid-continental rift of North America has abundant lava flows of Keweenawan age (~1 Ga) whose simple stratigraphy allow adequate assessment of paleo-horizontal. In this paper, we present new data from a study of the North Shore Volcanics along the shores of Lake Superior in Minnesota. We use these data to address the problem of elongation/inclination trends of PSV for the Keweenawan.

2. Geology and sampling

Fig. 2 shows the Bouguer gravity anomaly map compiled by the United States Geological Survey. The dark red area marks the Mid-continent rift structure which comprises one of the world's most extensive LIPs, stretching at least 2000 km from Kansas through Lake Superior. Bending south in eastern Canada, it terminates in the Grenville Front. Volcanism in the rift system spanned the interval from 1108 to about 1086 Ma (e.g., Davis and Green, 1997). An extrusive sequence known as the "Keweenawan Lavas" (after the Keweenaw Peninsula in northern Michigan) is exposed along the shores of Lake Superior, dipping roughly toward the lake. Although dominated by basaltic lava flows, the sequence also includes extensive felsic lavas and rheoignimbrites (Green and Fitz, 1993). The lava flow sequence is cut by many dikes, and is in places intruded by

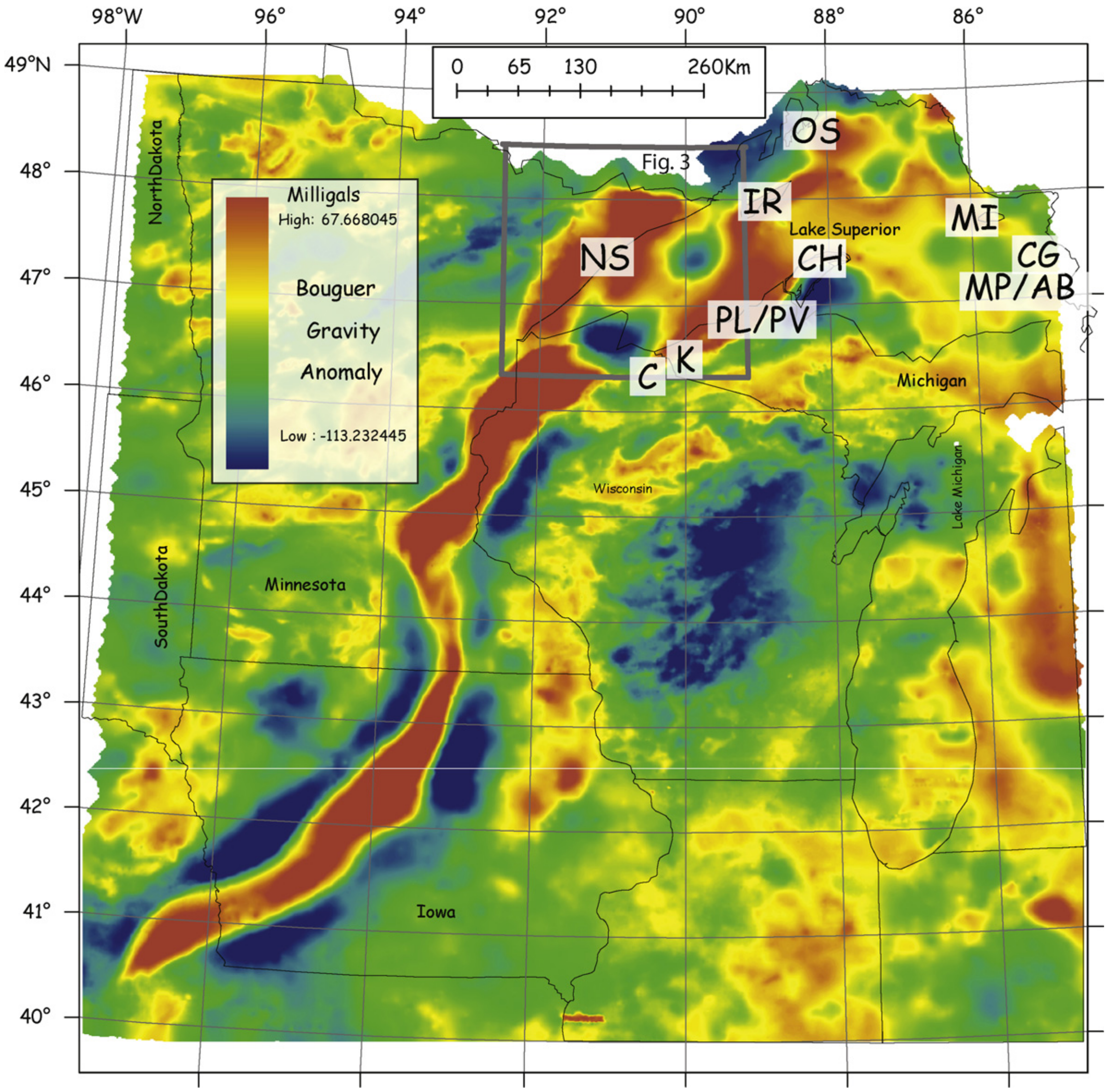

Fig. 2. Locations of studies on Keweenawan lavas (see Table 1). Basemap is gravity anomaly map modified from: http://www.geo.umn.edu/mgs/nicegeo/pdfs/boug_grav.pdf compiled by David L. Daniels and Stephen L. Snyder of the U.S.G.S. (For interpretation of the references to color in this figure legend, the reader is referred to the web version of the article.)

small granophyres (see, e.g., Vervoort et al., 2007). In Minnesota, the Midcontinent Rift lavas are in close association with extensive plutonic complexes that in places intrude into the lava sequences (see Fig. 2).

The Keweenawan lavas have been the subject of paleomagnetic and geochronologic study for decades (see Fig. 2 and Table 1). Since the comprehensive review by Halls and Pesonen (1982), there have been new studies, the most recent of which is the work of Hnat et al. (2006) on the Portage Lake Volcanics. This study showed that careful step-wise demagnetization of multiple specimens per lava flow was necessary to identify the primary component in the somewhat altered rocks, a procedure that was not done routinely in the earlier work. While of excellent quality, there were only 9 site means based on magnetite characteristic components available from the Portage Lake flows and additional data are necessary for testing the paleosecular variation model. We report here the results of a new study on the sequence of Keweenawan lava flows exposed along the North shore of Lake Superior between Duluth and Grand Portage in Minnesota, the so-called "North Shore Volcanics" in Table 1 and Fig. 3.

Miller et al. (2001) mapped four main sequences of basaltic lavas as shown in Fig. 3a: the Upper Southwest sequence, the Schroeder–Lutsen sequence, and the Upper and Lower Northeast sequences. The basaltic lavas of the North Shore Volcanics (NSV) have distinctive amygdaloidal flow tops in which are secondary minerals including the abundant agates that can be found in such places as "Agate Bay". There are numerous rhyolites, particularly in the Upper Northeast sequence, the thickest of which are shown in the map. The North Shore Volcanic sequences are intruded by diabase dikes and sills (e.g., Beaver Bay Complex and the Pidgeon River Diabase) and gabbros (e.g., the Brule Lake/Hovland Gabbro). The oldest flows are thought to be in the Lower Northeast sequence which are overlain by the Upper Northeast sequence. The youngest flows are in the Schroeder–Lutsen sequence. However, the exact age relationship between the Upper Southwest and the Upper Northeast sequences is not known exactly, but they appear to be approximately co-eval.

All four sequences have been sampled paleomagnetically by Books (1968, 1972) and Palmer (1970). Palmer (1970) documented 14 reversely magnetized "flows" in the Lower Northeast sequence

Table 1
Studies of Keweenawan lavas (see Fig. 2).

Code	Name	Lat.	Lon.	Ref.	Age (Ma)	Age ref.
AB/MP	Alona Bay/Mamainse Point	47	−84.5	Palmer (1970), Robertson (1973)		
C	Chengwatana Volcanic Group	46.5	−90.5	Kean et al. (1997)	1095	Zartman et al. (1997)
CG	Cape Gargantua	47.5	−85	Palmer (1970)		
CH	Copper Harbor Volcanics	47.5	−88	Halls and Palmer (1981)	1087	Davis and Paces (1990)
IR	Isle Royale	48	−89	Books (1972)		
K	Kallendar Creek Volcanics	46.7	−90	Palmer (1970), Books (1972, 1968)	1099–1107	Zartman et al. (1997), Davis and Green (1997)
MI	Michipoten Island	47.8	−86	Palmer (1970), Palmer and Davis (1987)	1086	Palmer and Davis (1987)
NS	North Shore Volcanics	47.5	−91	Palmer (1970), Robertson (1973), Books (1968)	1096–1100	Davis and Green (1997)
OS	Osler Group	48.75	−88	Palmer (1970), Halls (1974)	1098–1108	Davis and Green (1997), Davis and Sutcliffe (1985)
PL	Portage Lake Volcanics	46.8	−89.5	Books (1972), Browning and Beske-Diehl (1987), Hnat et al. (2006)	1094–1096	Davis and Paces (1990)
PV	Porcupine Volcanics	46.7	−89.5		1094	Zartman et al. (1997)

and 54 normal flows from the Schroeder–Lutsen and Upper Southwest sequences. Like Dubois (1962), Books (1968), and Palmer (1970) found that the normal and reverse directions were not antipodal, leading to much speculation regarding asymmetric reversals, overprinting or rapid plate motion (see, e.g., Pesonen and Nevanlinna, 1981).

The Upper Southwest sequence of the North Shore Volcanics (Duluth to Two Harbors) was described in detail by Sandberg (1938). Here the lavas strike between about 10° and 35° and dip to the south-east from about 20° to about 11° (Fig. 3a). North of Two Harbors to about 10 km southwest of Tofte, the lava flows strike parallel to the shoreline making suitable exposure scarce. Moreover, an extensive interval southwest of Tofte is quite complicated; it is heavily intruded by the Beaver Bay Complex, although there are some lava flows exposed there (e.g., the huge rhyolitic "Palisades Flow" of Green and Fitz, 1993). From Tofte to near Grand Marais, lava flows are again accessible along the shore line; these strike east-northeast and dip gently to the southeast between 12° and 15°. At Grand Marais, the lava flow sequence is interrupted by a sequence of red beds, dipping to the south at about 12°. From Grand Portage southward, we find the Lower Northeast sequence, which comprises the Grand Portage Lavas, intruded by dikes and sills of the Pidgeon River Diabase, the Brule Lake/Hovland gabbros and the Hovland lavas. These are overlain by the Upper Northeast sequence comprising the Marr Island Lavas, several extremely thick rhyolites (the Devil's Track to the south and the Kimball Lake to the north) with basaltic lavas sandwiched in between (The Croftville Volcanics). The rhyolites are intruded by dikes and sills, for example the Monker Lake diabase.

Rhyolites, granites, icelandites and granophyres from the Duluth Complex and NSV have been dated using U–Pb and zircons (Paces and Miller, 1993; Davis and Green, 1997; Vervoort et al., 2007). Vervoort et al. (2007) dated granophyres in the "hypabyssal rocks" which range in age from 1092 (Finland intrusion associated with the Beaver Bay Complex) to 1109 Ma (Whitefish lake intrusion). These dates are difficult to tie directly to the extrusive sequence which presumably predate them. Fortunately, Davis and Green (1997) dated rhyolites and an icelandite which are part of the extrusive section. Also, Paces and Miller (1993) published an age for the latest phase of the Beaver Bay Complex from near Beaver Bay, Minnesota of 1096 ± 1 which must post-date the North Shore Volcanics that it intrudes. These age constraints are summarized in Table 2 and

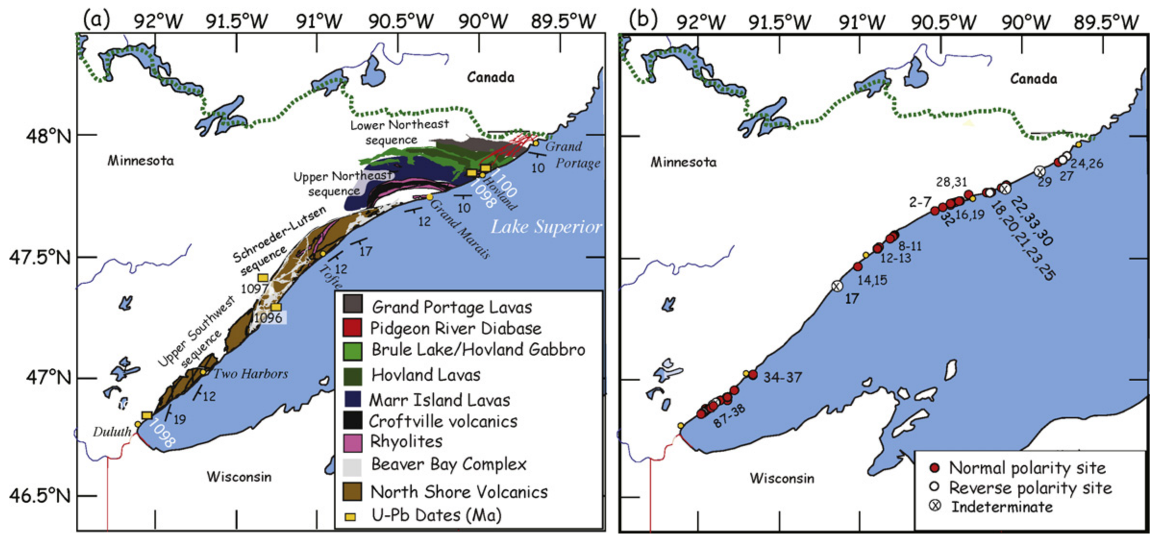

Fig. 3. (a) Geological map of four sequences of the North Shore Volcanics (based on Miller et al., 2001). U–Pb dates on rhyolite flows (numbers next to yellow squares) are from Davis and Green (1997) and Paces and Miller (1993) (see Table 2). (b) Sampling sites for this study (Tables 3–5). White circles are reversely magnetized while red circles are normal. Circles with an X were excluded from further consideration. Site 17 is in close association with roof rocks of the Beaver Bay Complex where the structure is complicated (see Miller et al., 2001). Other excluded sites had high within site scatter. (For interpretation of the references to color in this figure legend, the reader is referred to the web version of the article.)

Table 2
Age constraints.

Sample ID	Name	Lat.	Lon.	Age (Ma)	σ	Ref.
SBG2	Beaver Bay Complex—latest phase	47.25	−91.3	1095.8	1.2	Paces and Miller (1993)
DD88-4	40th Ave E. icelandite	46.82	−92.04	1098.4	1.9	Davis and Green (1997)
DD88-6	Palisade Rhyolite	47.33	91.22	1096.6	1.7	Davis and Green (1997)
MI-25	Devil's Kettle rhyolite	47.83	90.05	1097.7	1.7	Davis and Green (1997)
H-15	Big Bay rhyolite	47.84	89.97	1100.2	2.2	Davis and Green (1997)

Note: Locations are estimated from descriptions in the text.

in Fig. 3a. Please note that Davis and Green (1997) did not provide exact locations for their samples and we have estimated the locations from the maps and descriptions in the text. All the dates are statistically indistiguishable. However, the oldest flow appears to be the northernmost, north of Grand Marais (Big Bay Rhyolite, dated at 1100.2± 2.2 Ma). This interpretation could support the notion that the reversely magnetized lavas observed to the north of this unit found by Palmer (1970) are older than the normally magnetized flows to the southwest (see Halls and Pesonen, 1982).

For this study, we drilled 83 sites along the North Shore of Lake Superior and from outcrops along Route 61 (see Tables 3–5 and Fig. 3b). We drilled from 5 to 10 samples and oriented all of them with magnetic compass. Most were also oriented with a sun compass and these orientations were used if available. There was no significant difference between the magnetic and sun compass directions, however. Structural corrections were based on regional studies (see Fig. 3a) and confirmed by our own field observations. Samples were sliced into from one to three 2.5 cm specimens and measured with either a 2G or a CTF cryogenic magnetometer housed in the magnetically shielded room at Scripps Institution of Oceanography.

3. Paleomagnetism

Specimens from each site were subjected to step-wise alternating field (AF) and thermal demagnetization. Representative demagnetization curves are shown in Fig. 4. Median destructive fields (MDFs) ranged from less than 20 mT to well over 180 mT, the higher MDFs being associated with rhyolitic flows while the lower MDFs were associated with the basaltic flows. Those specimens that

Table 3
Summary of paleomagnetic data by site: magnetite remanences.

Site	Lat.	Lon.	D [a]	I [b]	L [c]	GC [d]	k [e]	D_{tc} [f]	I_{tc} [g]	λ_{tc} [h]	ϕ_{tc} [i]
NS004	47.73275	−90.43633	299.3	40.4	5	0	184.5	290	47.8	34	186.7
NS005	47.72542	−90.44299	305.3	29	4	0	298.6	299.8	37.6	35.3	172.4
NS006	47.7161	−90.49043	301.1	30.9	5	0	542.2	294.8	38.8	32.5	177
NS016	47.74304	−90.3824	291.4	50.6	4	1	72.7	277	56.1	30.5	202.1
NS019	47.74169	−90.39059	288.1	49.7	5	0	304.6	273.9	54.8	27.7	202.7
NS022	47.79647	−90.12863	307.1	32.5	4	1	254.3	301.3	38.1	36.5	171.8
NS026	47.91243	−89.75128	140.3	−56.6	5	0	521.9	126.2	−62.1	−52.9	13.8
NS027	47.90276	−89.77817	303.5	43.6	5	0	466.1	293.9	46.8	36	183.7
NS028	47.76711	−90.33177	295.9	26.7	5	0	505.9	288.6	32.7	25.5	178.4
NS031	47.76888	−90.33087	295.4	27	5	0	1314.5	288	32.9	25.2	179
NS035	47.01823	−91.65989	295	44	5	0	2377	293.8	55.9	41	191.2
NS037	47.02017	−91.65981	294.5	41.3	5	0	590.3	293.4	53.3	39.2	188.6
NS040	46.92496	−91.82067	290.2	39.6	5	0	598.1	289.5	55.6	37.9	193.3
NS041	46.92407	−91.81751	286.2	34.1	5	0	1321.2	284.5	50	31.4	191.2
NS043	46.90964	−91.86463	276.1	16.8	5	0	196.7	274	32.2	15.4	187.5
NS045	46.90995	−91.86348	275.1	15.4	4	0	1285.3	273	30.7	14	187.5
NS046	46.89996	−91.89156	302.2	27	4	0	171	304.4	42.8	41.1	171.5
NS048	46.89692	−91.89615	300.7	39.6	5	0	145.6	303.8	55.4	47.4	184.2
NS049	46.90292	−91.88615	299.9	38.4	4	0	175.6	302.6	54.2	45.9	183.6
NS050	46.88286	−91.91584	291.2	26.7	4	0	473.6	291.3	44.7	33.1	182.6
NS052	46.89534	−91.8985	294.8	38.2	4	0	180.8	295.8	54.2	41.3	187.9
NS053	46.87654	−91.93109	293.7	24.2	4	0	785	295.1	43	34.8	178.6
NS054	46.89499	−91.89934	290.2	40	4	0	150.5	289.5	56	38.2	193.7
NS056	46.89011	−91.90663	296.1	23.3	5	0	898.2	297.3	41.2	35.4	175.8
NS058	46.89011	−91.90663	302.2	34.9	3	1	158.3	306.1	52.5	47.4	179.2
NS059	46.8835	−91.91449	290.4	26.3	4	0	89.4	290.2	44.3	32.2	183
NS061	46.86879	−91.94866	300.4	31.4	4	1	237.9	304.5	49.8	44.8	177.4
NS062	46.86996	−91.94523	292.6	33.6	4	0	314.8	294.3	52.6	39.4	187.2
NS064	46.86785	−91.95036	296.4	29.4	4	0	253.6	298.9	48.1	40.1	179.9
NS065	46.86961	−91.94637	290.8	28.9	4	0	95.5	291.6	47.9	35	184.8
NS068	46.86433	−91.95615	310.8	16.1	4	0	127	314.5	33.4	43.1	156.2
NS071	46.8673	−91.95184	305.6	27.6	5	0	111.6	310.5	45.5	46.6	168.6
NS075	46.86576	−91.95402	302.4	33.1	5	0	175.8	307.6	51.3	47.8	176.7
NS077	46.86121	−91.96034	305.5	16.5	4	0	200.6	308.4	34.5	39.7	162.5

[a] Declination (geographic coordinates).
[b] Inclination (geographic coordinates).
[c] # of best-fit lines.
[d] # of great circles.
[e] Estimate of concentration parameter κ (Fisher, 1953).
[f] Declination (tilt corrected).
[g] Incination (tilt corrected).
[h] VGP latitude.
[i] VGP longitude.

Table 4
Summary of paleomagnetic data by site: hematite remanences. Superscripts for column headings same as Table 3.

Site	Lat.	Lon.	D^a	I^b	L^c	GC[d]	k^e	D_{tc} [f]	I_{tc} [g]	λ_{tc} [h]	ϕ_{tc} [i]
NS002	47.73415	−90.42919	291	32.6	4	0	191.1	283.5	38.7	24.9	185.2
NS006	47.7161	−90.49043	301.1	30.4	5	0	657	294.9	38.4	32.4	176.7
NS007	47.70123	−90.53907	307.4	31.8	5	0	173.2	301.5	40.6	37.9	172.9
NS008	47.60108	−90.78655	313.9	34	5	0	255.1	309.4	44.7	45.3	169.3
NS009	47.59789	−90.7915	291.5	41.6	4	0	400.8	281.9	49	29.3	192.7
NS010	47.59411	−90.79729	292.3	31.7	5	0	280.5	285.7	39.5	26.7	183.8
NS011	47.58531	−90.81521	293.8	19	5	0	249.8	290.1	27.2	24.1	174.3
NS012	47.54605	−90.89361	288.8	32.5	4	0	97.1	282.5	41.2	25.4	187
NS013	47.55097	−90.88284	290.5	29.2	4	0	444.3	285.2	38.2	25.8	183.4
NS014	47.46915	−91.01428	277.7	23.9	5	0	1478.5	272.8	31.7	14.4	188.8
NS015	47.46923	−91.0137	294.5	16.4	4	0	350.8	292	26.6	25.1	172.4
NS018	47.77667	−90.2093	312.6	5.5	5	0	71	311.4	12.2	31.4	150.7
NS020	47.77857	−90.19072	303.8	7.2	5	0	160.3	302.3	12.7	26.1	159.1
NS021	47.77705	−90.2205	311.6	21	5	0	903	308.1	27.5	36	160.1
NS023	47.77633	−90.20105	305.6	14	5	0	1001.5	303.1	19.6	29.4	161
NS024	47.92843	−89.72541	147.1	−69.7	4	0	462.2	120.2	−75.5	−54.5	47.1
NS034	47.01668	−91.66029	299.5	42.2	5	0	260.3	299.7	54.2	44	185.6
NS036	47.01631	−91.66031	297.5	42.6	3	1	197	297	54.6	42.4	187.7
NS039	46.95296	−91.77558	288.8	21.2	5	0	1425.8	287.6	33	25	178.3
NS044	46.91107	−91.86044	289.7	28.5	4	0	344	289.2	44.5	31.6	183.9
NS055	46.87575	−91.95249	284.3	17.7	5	0	390.5	283.6	36.7	23.9	182.9
NS060	46.86945	−91.94685	292.6	26.4	5	0	110	293.9	45.3	35.2	181.2
NS066	46.86674	−91.9526	313	19.7	4	0	1062.2	317.6	36.6	46.7	155.1
NS067	46.87085	−91.94296	287.5	28.6	4	0	299.2	287.4	47.6	32	187.3
NS078	46.85303	−91.97804	279.2	16.1	5	0	238.4	277.7	34.8	19	186.1
NS079	46.85781	−91.96647	285.7	30.5	1	3	963.9	285	49.5	31.4	190.4
NS080	46.8525	−91.97929	286.4	19.8	5	0	141.3	286	38.8	26.6	182.4
NS081	46.85641	−91.9705	277.2	32.9	5	0	115	273.3	51.4	24.9	199.2
NS083	46.85339	−91.97727	286.8	39.4	4	0	143.3	286.3	58.4	37.5	198.1
NS085	46.8528	−91.97874	280.5	19.3	5	0	383.7	279	38.1	21.5	186.9
NS087	46.85188	−91.98035	281.9	20	5	0	223.4	280.7	38.9	23	186.2

failed to reach their MDF with AF treatment (e.g., heavy red line in Fig. 4a) were subsequently treated to thermal demagnetization (e.g., heavy solid line in Fig. 4b). These all had blocking temperatures near 680 $^\circ$ suggesting a hematite carrier. The blocking temperature from all lava flows ranged from just under 600° to just under 700°.

A total of 235 specimens had less than 10% remanence remaining after demagnetization to 180 mT or at 600°. These we interpret as being dominated by magnetite. Examples of this type of behavior are shown in Fig. 5a and b for AF and thermal demagnetization, respectively. A further 196 specimens had more than 10% of the NRM remaining after treatment to these steps. These we consider significantly or completely contaminated by hematite. Examples of these are shown in Fig. 5c and d for AF and thermal demagnetization, respectively.

Regardless of remanence carrier, most sites were characterized by simple demagnetization behavior and excellent agreement of directions among the samples from the site (see Tables 3–5). Best-fit lines and maximum angle of deviation (MAD) were calculated through demagnetization data trending to the origin (insets to Fig. 5a–d using the method of Kirschvink (1980). Six sites had one or more specimen(s) whose demagnetization data was best interpreted as a great circle (see, e.g., Fig. 5e and f).

Average directions and cones of 95% confidence from directions with MADs $\leq 10^\circ$ from sites with only directed lines were calculated using the statistics of Fisher (1953). Data from sites with one or more great circle fits were combined using the method of McFadden and McElhinny (1988). All site means are listed in Tables 3–5.

Three sites had characteristic directions that were southeast and steeply up. These we interpret as being reversely magnetized. Examples of demagnetization behavior from representative specimens from these sites are shown in Fig. 6. The demagnetization data shown in Fig. 6a can be fit by two distinct components, a low-temperature component with a maximum unblocking temperature of about 300 $^\circ$C (demagnetization step 4 in the diagram)

Table 5
Summary of paleomagnetic data by site: mixed remanences. Superscripts for column headings same as Table 3.

Site	Lat.	Lon.	D^a	I^b	L^c	GC[d]	k^e	D_{tc} [f]	I_{tc} [g]	λ_{tc} [h]	ϕ_{tc} [i]
ns003	47.7371	−90.4114	296.7	41	5	0	414.1	286.9	47.9	32	188.9
ns017	47.3892	−91.1385	16.4	49.9	4	0	259.7	–	–	–	–
ns025	47.7763	−90.2011	133.9	−64	5	0	53.3	114.3	−69.7	−49.4	33.3
ns030	47.799	−90.1056	295.1	30.2	5	0	395.1	289.2	33.9	26.4	178.8
ns032	47.7319	−90.4429	293.4	33	5	0	285.9	286	39.7	27.1	184
ns038	46.9541	−91.7732	287.1	17.5	5	0	104.2	286	29.2	22.2	177.6
ns042	46.9105	−91.8175	291.6	27.1	5	0	104.5	291.6	43	32.4	181.2
ns047	46.9016	−91.8885	306.5	40.5	5	0	496.7	311.7	55.9	53.1	179.6
ns051	46.885	−91.912	292.9	24	5	0	224.5	293.3	42	33.1	179.3
ns057	46.8745	−91.9343	287.8	10.6	5	0	2270.1	287.7	29.6	23.5	176.4
ns063	46.8691	−91.9477	298	15.3	4	1	290.3	299.6	33.9	33.5	169.5
ns072	46.8584	−91.9653	290.5	35.2	2	3	236.1	291.5	54.2	38.4	190.6
ns073	46.8658	−91.954	305.4	16.5	4	0	82.1	308.4	34.5	39.7	162.5
ns074	46.8574	−91.9673	289.6	37.7	1	4	51.5	290.3	56.7	39.1	193.9

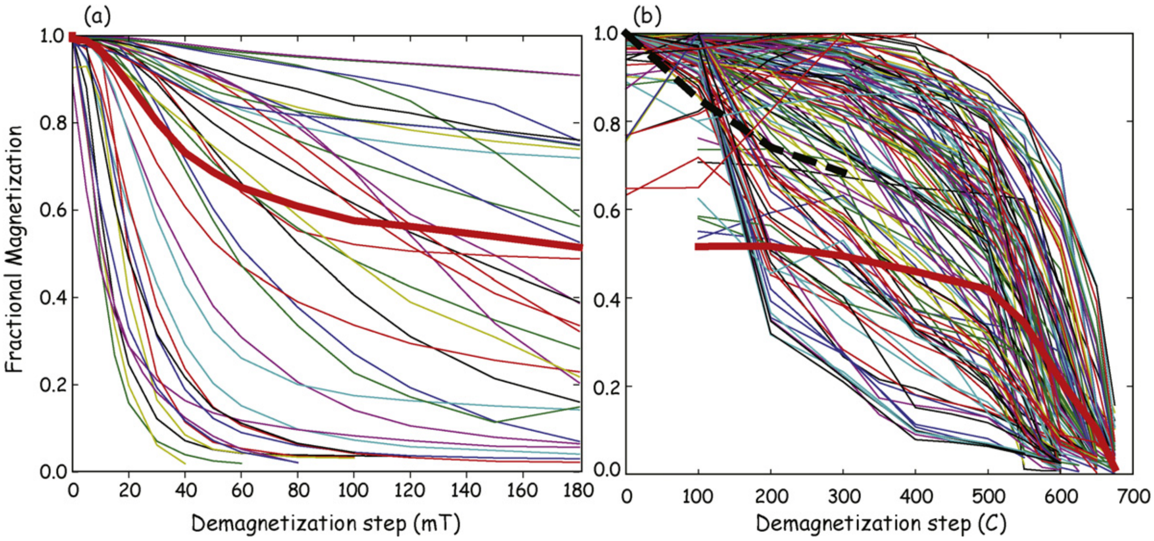

Fig. 4. Demagnetization behavior of representative North Shore specimens. Specimens with initial demagnetization steps of 100° (e.g., heavy solid line) had been demagnetized with AF to 180 mT (see heavy solid line in diagram to left) prior to thermal demagnetization. Specimens whose treatment stopped below 600° (e.g., heavy dashed line) exploded during thermal treatment.

and a high temperature component (steps 5–7) with a maximum unblocking temperature of less than 600 °C. These two directions are approximately antipodal (see Fig. 7) and the low-temperature component does not appear to be a present field overprint. Rather, it appears to be an overprint in a northwesterly and down direction.

Four sites behaved in an erratic fashion (see, e.g., Fig. 8). These had multiple components on demagnetization and poor within site consistency among specimen directions. No usable results were obtained from such sites. In addition to these poorly behaved sites, NS017 was taken just south of Little Marais in the Schroeder–Lutsen sequence (Fig. 3a). The outcrop is very near clearly overturned lavas that form the roof of the Beaver Bay Complex and its structural correction is difficult to constrain. We eliminate it from further consideration here.

A few sites had well clustered directions, with the exception of a single sample whose direction was displaced from the others (see specimen NS007b2 in Fig. 9a). There are several mistakes that occur occasionally in the field that can lead to misoriented directions. Many paleomagnetists simply throw out such deviant directions without further justification, a practice we find troubling. Instead, we follow Lawrence et al. (2009) who pointed out that the various common sources of misorientation in the field can be tested. For example, there are frequently stray marks on the sample which can be misinterpreted as being the orientation mark. Such a mistake would misorient specimen directions along a small circle about the specimen's "Z" direction (see Fig. 9b). The small circle of possible directions for specimen NS007b2 is shown as a dotted blue line in Fig. 9a. If the drill direction arrow were drawn in the wrong direction (out of the outcrop instead of in the direction of drill), the specimen direction would be the triangle in Fig. 9a. In the case shown here, it is quite plausible that a stray mark on sample NS007b was misinterpreted as the field arrow and the direction from the specimen from this sample (NS007b2) was discarded. Directions from a total of 15 samples were flagged as having "bad" orientations in this manner and were excluded from their respective site means.

There are a total of 78 sites with at least four specimen directions or great circles (with MAD angles $\leq 10°$) that had within site Fisher concentration statistics (k) of $\geq$50. We plot the directions of these in geographic coordinates in Fig. 10a and in tilt corrected coordinates in Fig. 10b. Structural corrections were taken from Miller et al. (2001). NS017 is shown in parentheses. The mean direction for the 74 (normal) sites (excluding NS017) meeting minimum criteria from the North Shore Volcanics is $D = 293$, $I = 43$ (see 'N' record labelled 'all' in Table 6 for details) and is similar to that published by Halls and Pesonen (1982). Also, we recovered three sites (NS024-NS026) that were reversely magnetized. As was noted by Palmer (1970) and others, these have directions that are steeper than the normal group ($D = 121$, $I = -69$, see 'R' record labelled 'all' in Table 6), an observation that led to much speculation about reversal asymmetry in the Keweenawan (e.g., Pesonen and Nevanlinna, 1981).

All of the data from this study have been uploaded into the MagIC database, including measurements, orientations, field photos and interpretations. The complete data set is available for downloading from earthref.org at this persistent link: http://earthref.org/cgi-bin/magic.cgi?mdt=m000629dt20090622093943.

Table 6
Summary statistics for various data sets.

Polarity	Component	$\bar{D}$	$\bar{I}$	N	R	k	α_{95}	E	E_{Dec}
N	All	293.0	42.8	74	72.1011	38.4	2.7	1.61	307.0
R	All	120.9	-69.1	3	2.9850	133.0	10.7	–	315.2
N	M	294.7	46.7	32	31.4047	52.1	3.6	1.13	264.3
N	Mixed	293.2	42.0	12	11.7683	47.5	6.4	2.9	276.4
N	M+	294.3	45.4	44	43.1432	50.2	3.1	1.52	274.2
N	H	291.4	39.0	30	29.0799	31.5	4.8	2.27	335.4

Components: M: magnetite; mixed: sites with directions based on magnetite and hematite specimen directions; H: hematite. M+ is magnetite plus mixed; $\bar{D}$: mean declination; $\bar{I}$: mean inclination; N: number of specimens; R: resultant vector length; k: Fisher's concentration statistic; α_{95}: Fisher's cone of 95% confidence (both from Fisher, 1953); E: elongation; E_{Dec}: elongation direction (both from Tauxe and Kent, 2004).

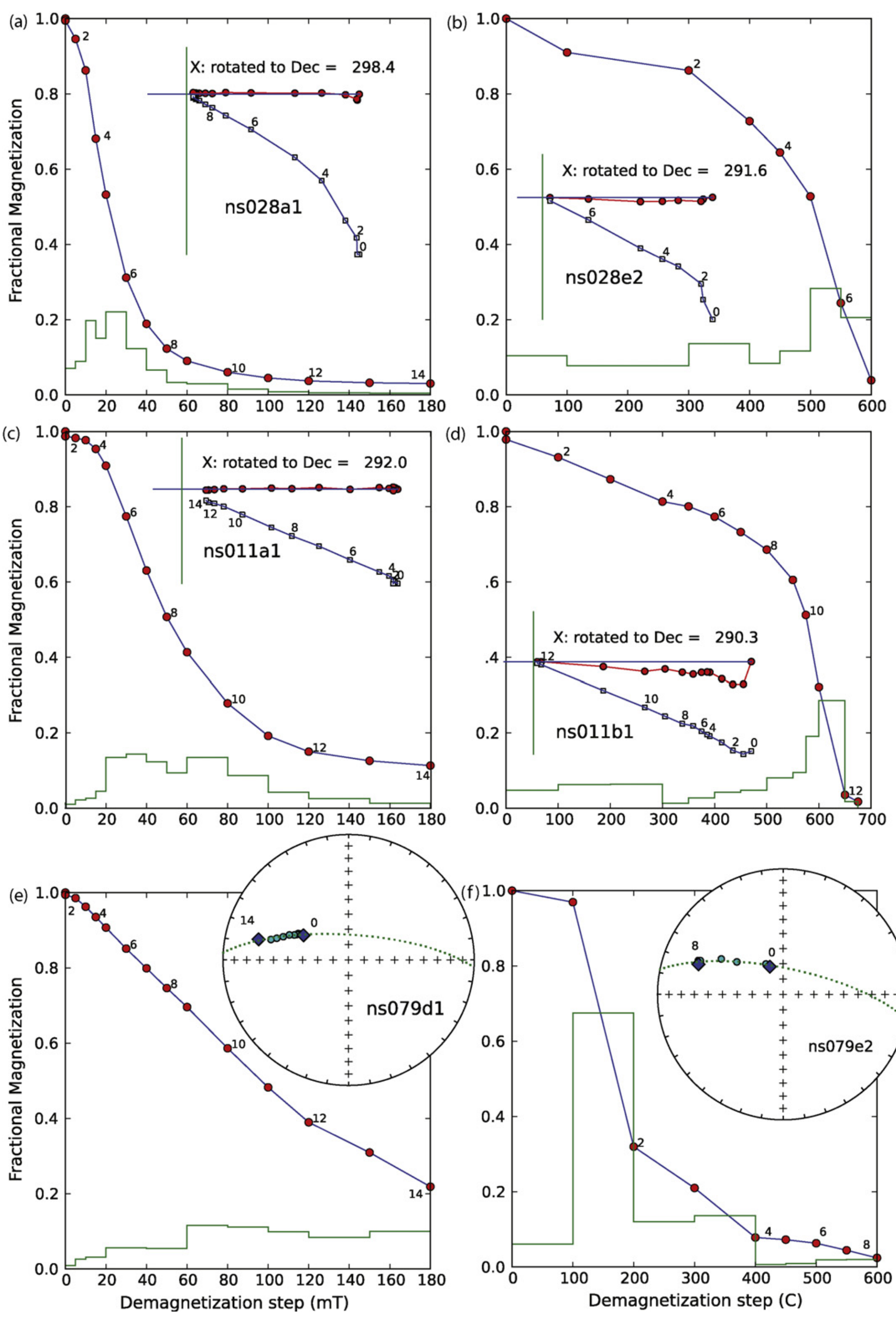

Fig. 5. Demagnetization behavior from representative specimens from the North Shore Volcanics. Left (right) hand panels are alternating field (thermal) demagnetization. Numbers are the demagnetization step numbers (0 is the natural remanence). Insets to (a)–(d) are vector endpoint diagrams (with horizontal X-axis rotated to specified angle). Circles are horizontal projection X, Y and squares are in the X, Z plane. (a and b) Less than 10% of the remanence remains after demagnetization to 180 mT (a) or 600 ◦ C (b), these specimens are classified as a "magnetite" remanence. (c and d) More than 10% of the remanence remains after demagnetization to 180 mT (c) and 600 ◦ C (d) so these specimens are classified as "hematite" remanences. Data shown in insets to (a)–(d) allow a simple best-fit line to be calculated to fine the characteristic direction. (e and f) Insets are equal area projections for demagnetization data with great circle fits shown as dotted lines (lower hemisphere projections).

4. Discussion

4.1. Origin and age of the magnetic remanence

As already mentioned, many of the specimens have remanences that are dominated by a magnetic carrier at a higher oxidation state than pure magnetite (here called loosely "hematite"). Here we consider the possible effect of secondary overprinting on our Keweenawan results. Many sites have both types of specimens and many specimens exhibit a drop in remanence between 550 and 600◦ (typical of magnetite) but continue to demagnetize up to between 650 and 700◦ (typical of hematite). In these cases, we

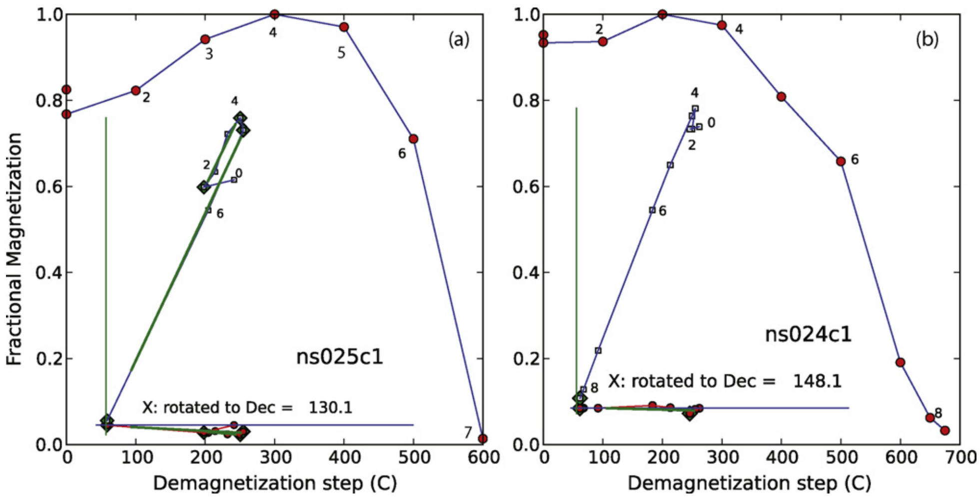

Fig. 6. Same as Fig. 5, but for reversely specimens. (a) Magnetite remanence with two components, one fit through steps 2–4 and one fit through steps 5–7. These directions are shown in Fig. 7. Note that the direction of the X-direction of the vector end-point diagram (130.1° is shown in Fig. 7 as a red line). (b) Hematite remanence.

could discern no change in direction of the components carried by magnetite and hematite. We list site means based solely on magnetite remanences in Table 3, those based solely on hematite remanences in Table 4 and those based on "mixed" remanences in Table 5. One site had at least four specimens with both magnetite and hematite dominated remanences, allowing a separate calculation of site mean for both types: NS006. The two site mean directions differed by only 0.5°.

Similarities at a site and specimen level notwithstanding, the magnetite and hematite directional groups could be significantly different from each other. We plot site means based solely on magnetite ('M') and those based solely on hematite remanences ('H') in Fig. 11a and b, respectively. Sites means not included in either the magnetite or hematite plots, with both types of remanences ('mixed') are shown in Fig. 11c. Mean directions and Fisher statistics (Fisher, 1953) are listed in Table 6 separated into normal (N) and reverse groups (R) and labelled 'M', 'H' and 'mixed', respectively.

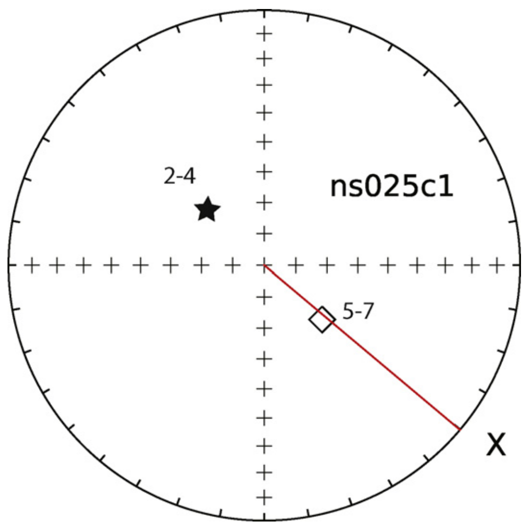

Fig. 7. Data from specimen ns025c1. These are the component directions for the two components in Fig. 6a. The low temperature component (steps 2–4) with a maximum unblocking temperature of 300 °C is nearly antiparallel to the high temperature (magnetite) component with a maximum unblocking temperature of less than 600 °C. The directions of the X-axis of the vector end-point diagram in Fig. 6a is shown as the red line. (For interpretation of the references to color in this figure legend, the reader is referred to the web version of the article.)

The two directional groups here called "magnetite" and "mixed" are indistinguishable from one another at the 95% level of confidence (Table 6). For this reason, the 'mixed' sites can be combined with the magnetite only sites and statistics on the combined data set are labelled M+ in Table 6. However, the difference between the "magnetite" and "hematite" groups is a little more problematic. In fact, these two groups fall in the awkward category whereby the cones of 95% confidence (α_{95} s in Table 6) overlap but do not include the other mean. There are several ways of testing for common mean under these circumstances, most of which require the assumption that the directions were drawn from a Fisher distribution (see McFadden and McElhinny, 1990, for a discussion). Paleomagnetic directions are frequently not Fisherian (e.g., Tauxe et al., 1991) and some form of non-parametric approach would be helpful. Here we use the bootstrap test for a common mean direction between the magnetite and hematite data sets developed by Tauxe et al. (1991) in the slightly modified form described by Tauxe et al. (1991). This test addresses the question "can the means of two data sets be discriminated from one another?" without relying on the assumption that directions are distributed according to a Fisher distribution (Fisher, 1953).

To carry out the bootstrap test, we draw random samples of data points (with replacement) and calculate a mean direction. This is repeated a number of times (here 5000). The 5000 bootstrapped mean directions for each group are shown in Fig. 12a. Each mean is then converted to Cartesian coordinates (X, Y, Z). Cumulative distributions of the components for the bootstrap means of the two directional groups are shown in Fig. 12b–d along with the bounds containing 95% of each component for the two groups. The null hypothesis that two data sets have a common mean direction can be rejected if any of the three components are different at the 95% level of confidence. For the magnetite and hematite data considered here, both the Y and Z components are significantly different; hence the magnetite and hematite directional groups do not share a common mean direction. This conclusion also applies to the 'magnetite' plus 'mixed' group of directions with respect to the hematite only directions. Therefore we consider that the hematite dominated sites have directions dominated by a secondary overprint and exclude them from further discussion of the ancient magnetic field.

In addition to the usual Fisher statistics for site means, we also include the elongation E and its direction E_{Dec} in Table 6. Those data

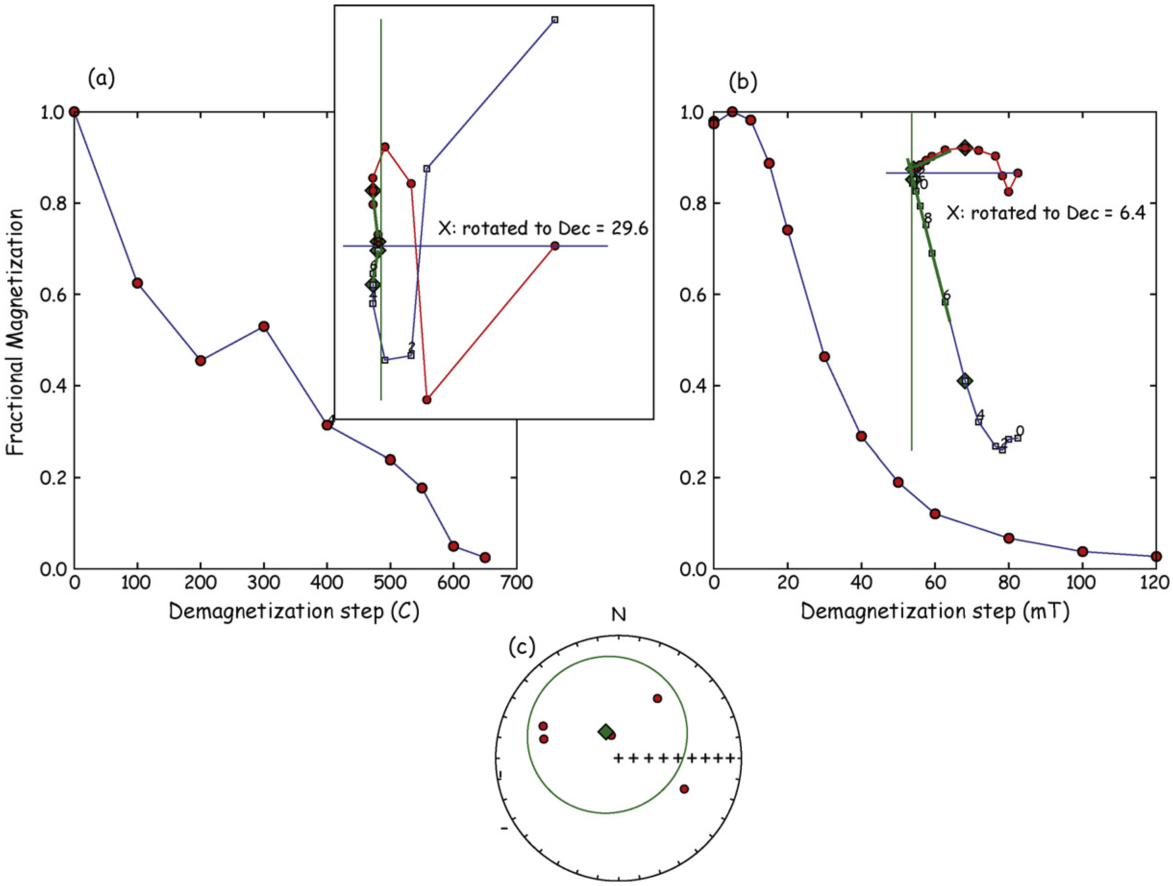

Fig. 8. Data from site NS076 as example of behavior typical of a sites with estimated Fisher precision parameters less than 50. (a) Thermal demagnetization as in Fig. 5a. (b) Alternating field demagnetization as in Fig. 5b. (c) Equal area projection for site. The data are highly scattered with an estimated precision parameter of 3.

sets excluding the hematite dominated sites have elongation directions in the plane of the mean direction, as expected from vectors with a geomagnetic origin. However, those data sets that include the hematite dominated sites, E_{Dec} is significantly deflected consistent with the hypothesis that these directions do not sample the same geomagnetic field.

4.2. Reversal asymmetry

The asymmetry in normal and reverse directional groups observed here (Table 6) has been known for decades. Dubois (1962) documented two groups of directions from what he called the Logan dykes and sills, Groups I and II. Group I directions had a mean

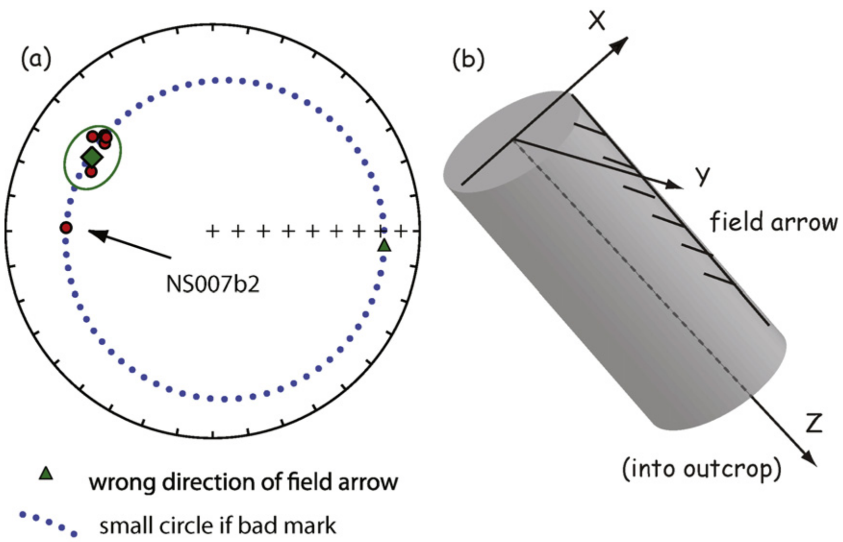

Fig. 9. (a) Sample orientation. (b) NS007 specimen directions in geographic coordinates. Predicted directions from specimen NS007b2 using two common mistakes. (For interpretation of the references to color in this figure legend, the reader is referred to the web version of the article.)

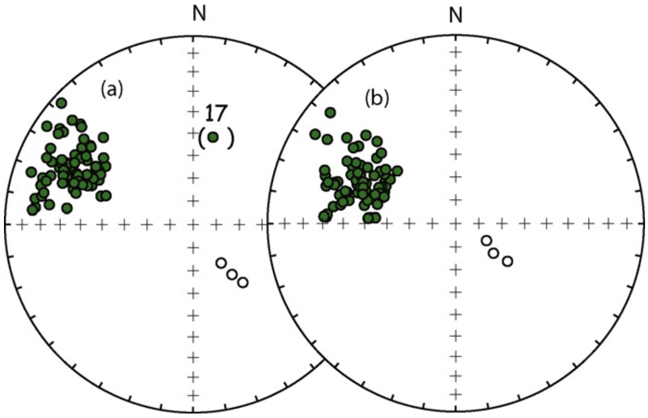

Fig. 10. Data from all site mean directions with $k \geq 50$ and $N \geq 4$ using all specimens from the site that met minimum criteria. Solid (open) symbols are in the lower (upper) hemisphere, plotted in equal area projection. (a) Geographic coordinates. (b) Tilt corrected coordinates.

of $D = 117$, $I = -76$, $k = 13.2$, $N = 80$ and Group II had a mean of $D = 288.5$, $I = 47.5$, $k = 21.1$, $N = 25$. This paper was remarkable in that it predated the pioneering work of, e.g., Cox et al. (1963) in arguing strongly for the fact that the magnetic field reversed its polarity. Secondly, Dubois (1962) argued that Group I was associated with the Logan sills while Group II came from what is now mapped as the Pigeon dikes (Miller et al., 2001). He observed places where the latter intruded the former, arguing that the two directional groups were of different ages. From the description of sampling sites, his Group I directions were taken in a swath of dikes and sills from what is now mapped as Nipigon sills to the Logan Sills and associated dikes south of Thunder Bay while many of his Group II directions appear to be taken from the Pigeon river dikes. Books (1968) followed up on the work of Dubois (1962) and sampled lavas from the Portage Lake Volcanics in Michigan and the Grand Portage lavas in Minnesota. His mean direction for the Grand Portage lavas, based on 11 flows south of Grand Portage, MN was $D = 117$, $I = -59.2$, $k = 129$, consistent with our reverse mean (see Table 6). Moreover, his mean for the Portage Lake lavas ($D = 289$, $I = 35$, $k = 106$, $N = 29$) is also consistent with that found by Hnat et al. (2006). Beck (1970) and Palmer (1970) summarized and expanded on the paleomagnetic results from the intrusive and extrusive Keweenawan sequences, respectively. They confirmed the general findings of both Dubois (1962) and Books (1968). But while Beck (1970) interpreted the different directions as the result of polar wandering, Palmer (1970) argued on the basis of a conglomerate test that the asymmetry of the normal and reverse groups was the result of a secondary overprint in a shallow westerly direction. Such an overprint would make the Group I directions steeper and the Group II directions shallower. His preferred pole position for the Middle Keweenawan was an average of the two. Robertson and Fahrig (1971) reprised the earlier work of Dubois (1962) and found that the Logan sills were mostly normally magnetized while the dikes (Pigeon River and on the Sibley Peninsula) were reverse (Group I). They treated the specimens with thermal demagnetization and found the same two non-antipodal sets of directions as Dubois (1962). They found no evidence of overprinting as the cause of the asymmetry in their demagnetization experiments. Arguing for an age progression, Robertson and Fahrig (1971) defined the Logan Loop of the North American apparent polar wander path, a view expanded upon by Robertson (1973) in a study of the Keweenawan lavas on Mamainse Point. Pesonen and Nevanlinna (1981) reviewed the arguments for overprinting laid out chiefly by Palmer (1970) and Palmer et al. (1981) and age progression by Robertson and Fahrig (1971) and Robertson (1973). They also considered various scenarios in which the time averaged field is not that of a geocentric axial dipole. They concluded that an oscillating co-axial two dipole model could explain the available data.

The three general explanations for the reversal asymmetry: polar wandering, overprinting and long term non-dipole field behavior have been revisited ever since with most studies favoring polar wander as the explanation (see, e.g., Halls and Pesonen, 1982; Schmidt and Williams, 2003; Borradaile and Middleton, 2006; Li et al., 2008). Although we cannot resolve the issue of asymmetric reversals with our three reverse sites, we did find the story to be somewhat more complex than the simple division into Upper and Lower North Shore groups. There is a reversely magnetized flow (NS025) with a mixed remanence within the Upper Northeast sequence (likely to be in the Monker Lake Diabase) and a normally magnetized (magnetite remanence) unit in the Lower Northeastern sequence (NS027). NS027 was taken from the Brule Lake/Hovland Gabbros. NS026 (reverse magnetite remanence) was taken from the Deronda Bay Andesite and NS024 (reverse hematite remanence) was taken from the Portage River Basalts. Our average reverse direction (Table 6) is quite similar to the Group I direction found previously, so it is not a mere fluke of undersampled secular variation. Although all three reverse directions are fairly similar,

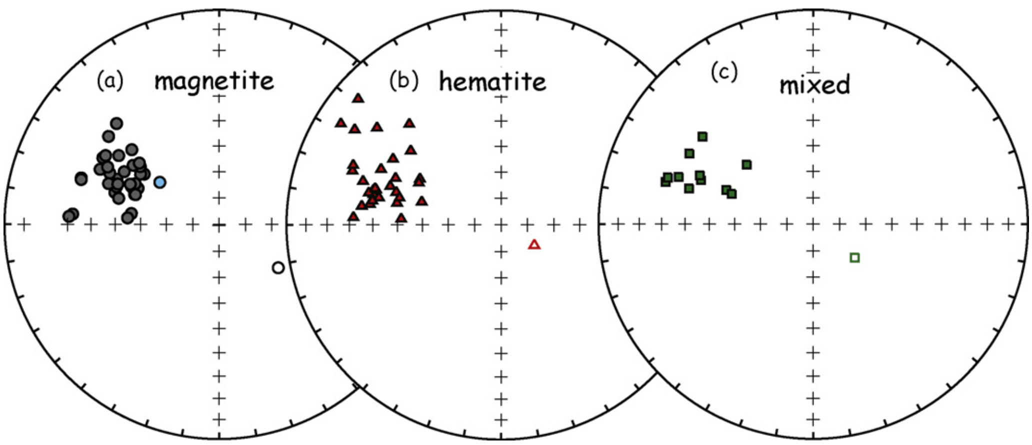

Fig. 11. Data from all acceptable site mean directions using specimens from the site that met minimum criteria for various magnetic mineralogies. Solid (open) symbols are in the lower (upper) hemisphere, plotted in equal area projection. Data are in tilt corrected coordinates. (a) Site means based solely on "magnetite" remanences (see Table 3). Light blue dot is the antipode of the sole reverse site (NS026) based on magnetite remanence directions. (b) Site means based solely on "hematite" site means (see Table 4). (c) Site means for sites not included in (a) or (b) that were based on both hematite and magnetite specimen remanences (see Table 5). (For interpretation of the references to color in this figure legend, the reader is referred to the web version of the article.)

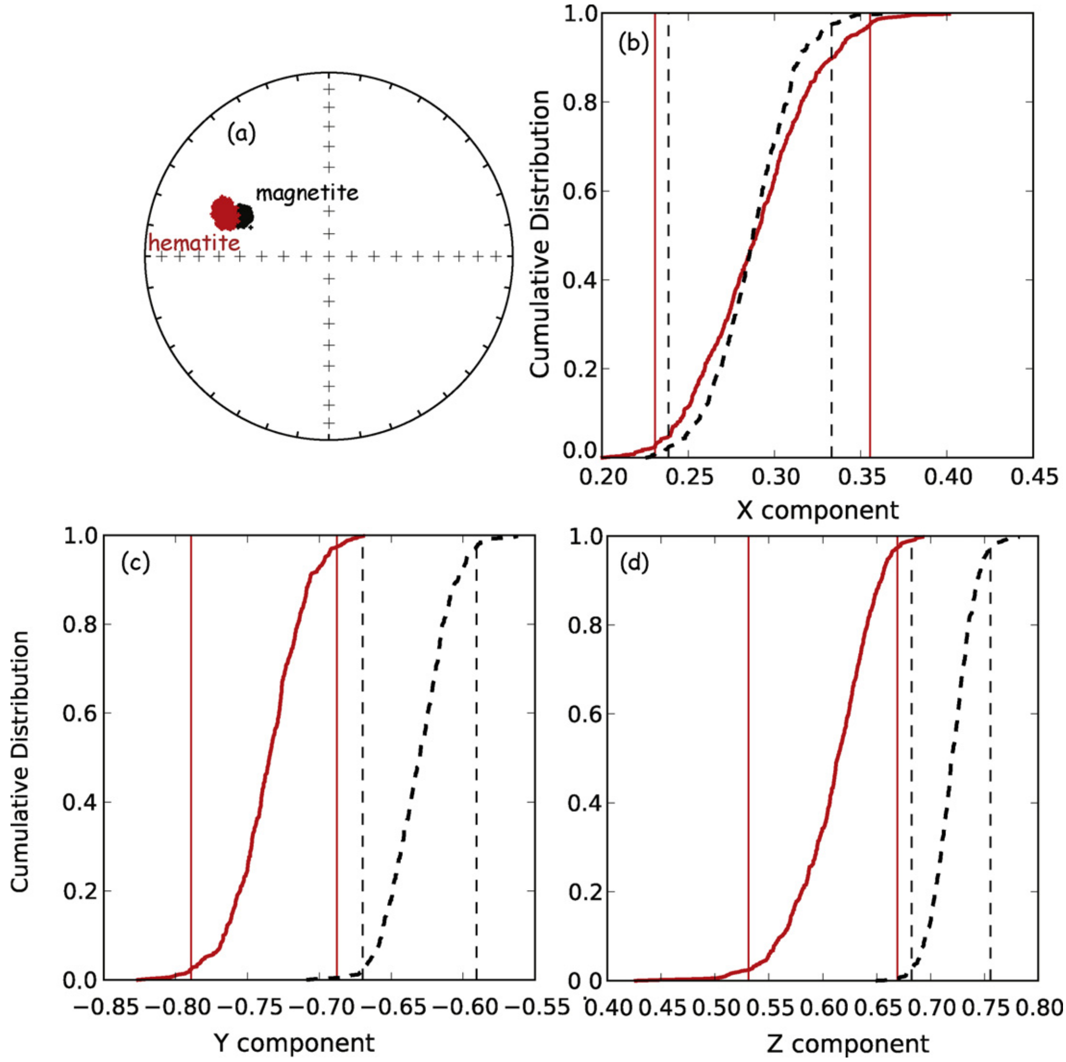

Fig. 12. (a) Distribution of means of 5000 bootstrapped pseudo-samples of the magnetite (black) and hematite (red) directions shown in Fig. 11a and b, respectively. (b–d) Cumulative distributions of Cartesian components of means shown in (a) with solid red lines being the hematite and dashed black lines the magnetite directions, respectively. The bounds containing 95% of the values for each set of components are shown as solid and dashed lines, respectively. (b) X components. These are indistinguishable between the two groups. (c) Y components. The two groups are different at the 95% level of confidence. (d) Z components. These are also different at the 95% level of confidence. (For interpretation of the references to color in this figure legend, the reader is referred to the web version of the article.)

the one based solely on hematite is the steepest (NS024 in Table 4) and the one based solely on magnetite is the shallowest (NS026 in Table 3). Following the logic of, e.g., Palmer (1970), if the primary reverse direction were overprinted in the hematite overprint direction (shallow and to the west), the reverse direction would become steeper. The fact that the NS026 direction is compatible with the other magnetite remanences (Fig. 11a), while NS024 and NS025 are steeper seems to argue in favor of a steepening caused by overprinting the hematite direction.

4.3. Models of PSV

Since the introduction of Model G for PSV by McFadden and McElhinny (1988), it has been customary to describe PSV in terms of scatter of the data after conversion of each direction into an equivalent virtual geomagnetic pole (VGP). VGP scatter is thought to depend on latitude which in and of itself provides clues to the origin of paleosecular variation in terms of dipole and quadrupole family sources. Yet this treatment assumes that paleolatitude is known *a priori*. Moreover, Model G is not a statistical field model and only describes the average trend of VGP scatter with latitude, hence it is of little use for predicting distributions of directions as required for discriminating among the various possible causes for shallow inclination bias in the paleomagnetic literature.

Statistical PSV models, starting with the CP88 model of Constable and Parker (1988) can predict directional distributions. We plot the elongation/inclination trends predicted from the GAD version of the TK03 model as a solid line and the TK03.g30 model as a dashed line in Fig. 13. Tauxe et al. (2008) calculated the elongation/inclination pairs for a number of large igneous provinces (LIPs) and these are shown in gray in the figure. We here also include the results of Rochette et al. (1998) from the Oligocene aged Ethiopian traps which were not included in the study of Tauxe et al. (2008).

To estimate the uncertainties, we follow Tauxe et al. (2008) who calculated the elongations and inclinations for a large number of bootstrap pseudo-samples (here we use 5000). The elongation/inclination pair for the (normal) magnetite (including sites based on 'mixed' remanences) directions and the bootstrap confidence bounds are plotted in black in Fig. 13. The hematite directions may have been biased by an overprint and we are reluctant to use them for a PSV study. It appears that the data from the large igneous provinces, including the Keweenawan are in reasonable agreement with the elongation/inclination trend predicted from the TK03.GAD PSV model.

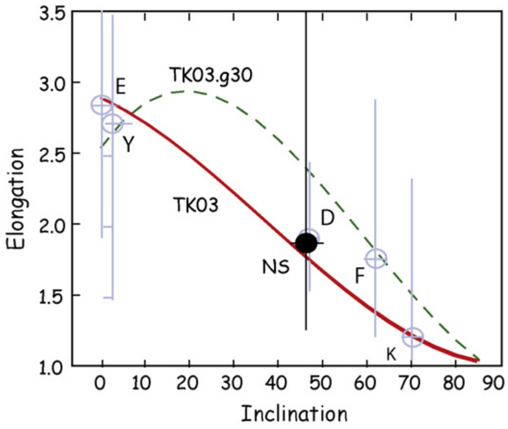

Fig. 13. Elongation/inclination curve of the TK03 model (Tauxe et al., 2005) shown as solid red line. TK03.g30 (20% octupole contribution) is the dashed green line. Data from large igneous provinces compiled by Tauxe et al. (2008) shown as light blue. Y: Yemen (28–30 Ma); D: Deccan (65 Ma); F: Faroe (55–58 Ma); K: Kerguelen (24–30 Ma). Also shown are the ~30 Ma data from the Ethiopian traps (E) of Rochette et al. (1998). The results from the Keweenawan lavas of this study are shown in black and are marked "NS". (For interpretation of the references to color in this figure legend, the reader is referred to the web version of the article.)

Here we plot the elongation/inclination trend predicted from the TK03 model if there were such a non-zero axial octupolar contribution (dashed line in Fig. 13). Distributions of directions generated by the TK03.g30 PSV model are much more elongate than those produced by the GAD model for inclinations between 20 and 80°. In general, the data sets from large igneous provinces, including the North Shore data presented here are quite consistent with the GAD model and are less well fit by the model including a non-zero average of the axial octupole. The only exception is the data set from the Faroe Islands which plots closer to TK03.g30 than to TK03.GAD.

From the foregoing we conclude that the elongation/inclination trend predicted from PSV models based on the last 5 million years is reasonably robust and may be used to detect and correct inclination bias in Neoproterozoic aged sediments. Moreover, it appears that large octupolar contributions are incompatible with most of the data sets.

4.4. *Frequencies of inclination data in the Paleozoic and Pre-Cambrian*

Given the fact that we find no compelling evidence for large, permanent non-GAD contributions to the field even as far back as the Keeweenawan, it is worth re-considering some of the analyses

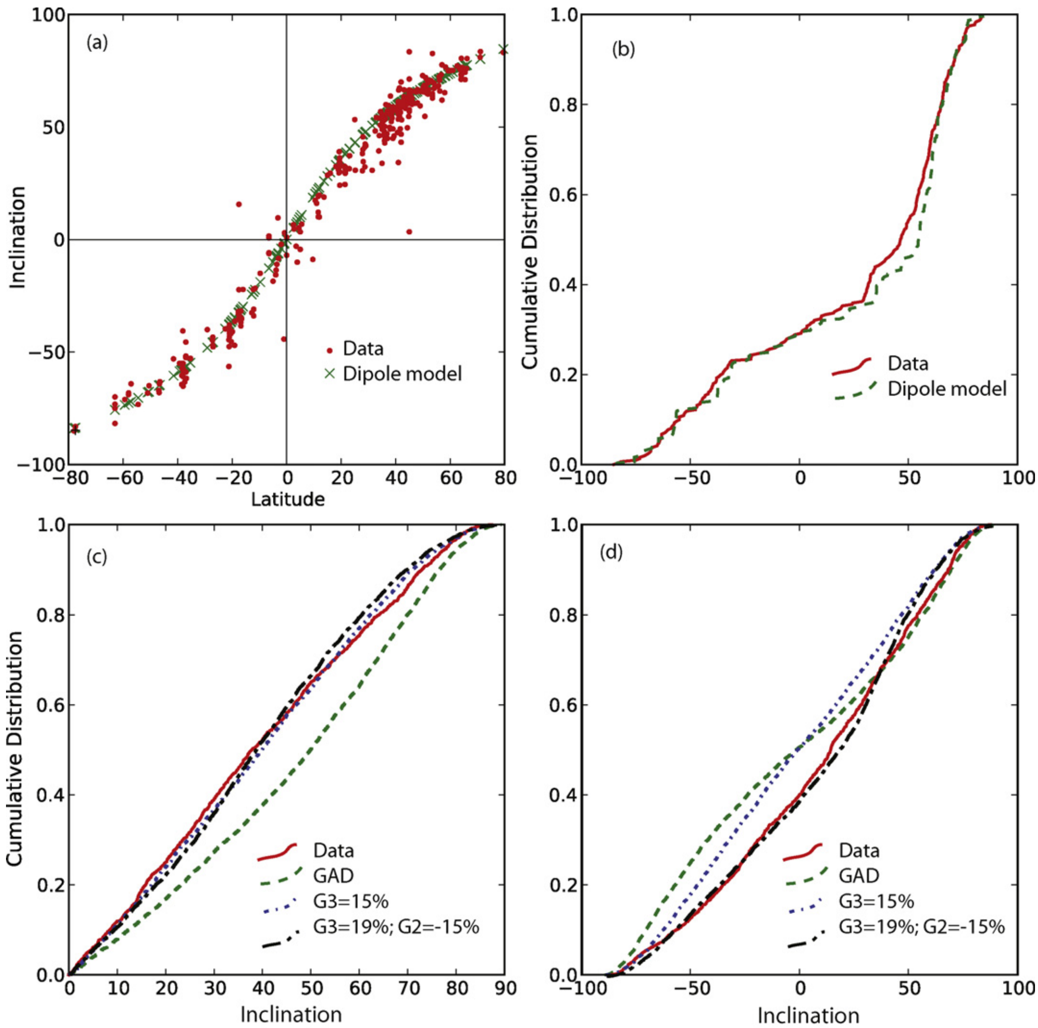

Fig. 14. (a) Inclination versus latitude for 0–5 million years poles obtained from the GPMDB (see text). Red dots are the data and green X's are from a GAD field model. (b) Cumulative distribution of inclinations plotted in (a). (c) Cumulative distribution of absolute values of inclinations from poles older than 250 million years from the GPMDB (solid line) versus those expected from a random sampling of a GAD field (dash line). (d) Same as (c) except not absolute values. (For interpretation of the references to color in this figure legend, the reader is referred to the web version of the article.)

that have been used to bolster arguments in favor of a non-zero axial octupole contribution in the Paleozoic and Pre-Cambrian. In particular, Kent and Smethurst (1998) examined the distribution of average inclinations from pole positions drawn from the Global Paleomagnetic Database (GPMDB) of McElhinny and Lock (1996). In order to compensate for unequal coverage in time and space, they averaged data in $10^\circ \times 10^\circ$ bins by age and plotted histograms of the frequencies of the absolute values of the inclinations. They concluded that while the Mesozoic and Cenozoic frequency plots were reasonably close to that expected from a GAD field, those from the Paleozoic and Pre-Cambrian were not. Possible reasons for the discrepancies were that the more ancient data sets did not have good coverage of the globe because the continents lingered at the equator, complications in the binning procedure which could have combined data from different tectonic blocks together in the average, or an average axial octupole contribution of some 20% of the dipole (G3 = 20%).

Because of the inherent difficulties in binning of data both in spatio-temporal bins and as histograms, we take a different approach here. First, we consider the case in which we can neglect plate motion (poles younger than about 5 million years). The GPMDB was migrated to the Norwegian Geological Survey (NGS) website: http://www.ngu.no/geodynamics/gpmdb/ in February, 2005. We retrieved a list of all poles from igneous units younger than 5 million years. We plot inclinations calculated from the poles against the latitudes of the sampling sites as red dots in Fig. 14a. Also shown are the inclinations predicted for those latitudes from a GAD field (crosses). The pattern is of course quite similar to that found in every study since Opdyke and Henry (1969). In Fig. 14b, we plot the inclination data as a cumulative distribution (solid line). This type of plot is similar in many ways to histograms but avoids the necessity of binning the data. Also shown is the cumulative distribution of the inclinations expected from random sampling over the globe of a GAD field (dashed line). A Kolmogorov-Smirnov two sample test compares the distribution of one data set to another and estimates the probability that the two data sets were drawn from the same underlying distribution. When applied here, this null hypothesis can be rejected at the 95% level of confidence. As has been noted since Wilson (1970), the inclination data are better fit with the inclusion of some permanent contribution of the non-dipole field. The inclusion of as little as 1% non-zero axial quadrupole (G2 = 1%) makes the two data sets compatible, however.

Applying this methodology to earlier times is problematic as any definition of paleolatitude requires a GAD assumption. This was the primary rationale for plotting frequencies of inclinations and comparing them to those expected from a uniform sampling of the ancient magnetic field (see, e.g., Evans, 1976). For the present re-analysis, we retrieved a list of all poles from igneous units older than 250 Ma from the NGS website. Kent and Smethurst (1998) plotted frequencies of the absolute values of the inclinations, so we first plot the absolute values of the inclinations in Fig. 14c. We also show a plot of the inclinations which would be observed from a random sampling around the globe of a GAD field (dashed line). These two curves are of course quite different with data being skewed toward shallower directions as noted by Kent and Smethurst (1998). We found a reasonable fit to these with G3 = 15% (the fit with 20% as suggested by Kent and Smethurst (1998) failed at the 95% level of confidence).

Because the axial octupole term is asymmetric about the equator, however, treating only the absolute values of the inclinations poses a serious problem. In fact, a strikingly different picture emerges when we consider the inclinations themselves and not the absolute values. These are plotted in Fig. 14d. Here we see that the data are very poorly fit by a random sampling of a GAD field (compare the solid and dashed lines). Moreover, a comparison of the inclinations with those predicted by a non-GAD field with G3 = 15% failed the K–S test at the 95% level of certainty. In fact we could find no simple field (varying only G2 and G3) that could fit the data. Our best-fit model is with G2 = −15 and G3 = 19% (long dash-dot line in Fig. 14c and d) but the agreement between model and data was poor. Of course we could find a field model that fit the observations exactly but these models become increasing *ad hoc*. Given the results of our re-analysis of the GPMDP pole data, it seems most likely that the failure of the inclinations to fit a model of random sampling of a GAD field is not the GAD field assumption but rather the random sampling assumption, a possibility discussed by Kent and Smethurst (1998) (see, also Meert et al., 2003).

5. Conclusions

(1) As in earlier studies of the North Shore Volcanics (e.g., Books, 1968; Palmer, 1970), we find two main directional groups in the North Shore Volcanics: a normal direction that is shallow and to the west and a reverse direction that is steep and to the southeast. These directions are the same as those found initially by Dubois (1962) in the Pigeon River Dikes and the Logan sills, respectively.

(2) Scrutinizing the demagnetization data in more detail reveals that the magnetization of the North Shore Volcanics can be attributed to both magnetite and hematite directions. We have classified site mean directions into three groups: those that were based on magnetite directions solely, those that were based on hematite directions solely and those that had specimens with both types of remanence (here called "mixed"). While the "magnetite" and "mixed" site means are indistinguishable, the magnetite and hematite site means do not share a common mean, with the hematite direction being significantly shallower. The magnetite directions are significantly steeper than the hematite directions, and are intermediate between the reversely magnetized directions and the hematite components. The three magnetite directions are fortuitously based on all three magnetizations with the hematite direction being the steepest and the magnetite direction being the shallowest. The antipode of the latter is compatible with the other magnetite directions. We interpret these results as support for the hypothesis that the asymmetry in normal and reverse directions in the Keweenawan data sets stems from overprinting in the shallow westerly direction.

(3) While there are substantial differences among the statistical (Giant Gaussian Process) paleosecular variation models, all predict distributions of directions that are circular at the poles where the average directions are near vertical and elongate in the meridian near the equator where the directions are near horizontal. Here we test whether the directional data from the North Shore Volcanics are consistent with the PSV model of Tauxe and Kent (2004) (see also Tauxe et al., 2008). Of particular interest is whether a field with a strong non-zero octupolar term can be excluded. Elongation (defined as the ratio of the intermediate and minimum eigenvalues of the orientation matrix of the directions) in the TK03.GAD when plotted against inclination defines a smooth trend, allowing a given data set to be tested against the distribution predicted by the field model. Excluding the sites based solely on hematite remanences, there are 44 site means that we consider to represent "primary" directions from lava flows in the North Shore volcanic group. From these we calculate the average inclination and elongation; these are compatible with those predicted by the TK03.GAD statistical paleosecular variation model. Moreover, a field model with significant non-zero octupolar contributions provides a much less convincing fit.

(4) A re-analysis of the treatment of inclinations from the Global Paleomagnetic Database shows that the data are very poorly fit by a random sampling of a GAD or simple non-GAD field. It is more likely that the existing database significantly undersamples the field in a spatial sense, as discussed by Kent and Smethurst (1998) and Meert et al. (2003).

Acknowledgements

We are grateful for the cheerful field assistance of Ryan Miller, Elise Sbarbori, Katharine Turkle, and Daniel Staudigel. Thanks are owed to Curtis Gagnon and Norman de Schampe of the Grand Portage Reservation for allowing us to sample on their land. Samples were measured by Ryan Fields, Katharine Turkle and Jason L. Steindorf. We have benefitted from many discussions with Jeff Gee and Dennis Kent. Two anonymous reviewers significantly improved the manuscript—you know who you are! Partial funding was provided by the Academic Senate of the University of California and NSF grant # ANT 0538392 to LT.

References

Beck, M.E.J., 1970. Paleomagnetism of Keweenawan intrusive rocks, Minnesota. J. Geophys. Res. 75, 4985–4996.
Books, K., 1968. Magnetization of the lowermost Keweenawan lava flows in the Lake Superior area. USGS Prof. Pap. 600-D, D248–D254.
Books, K., 1972. Paleomagneitsm of some Lake Superior Keweenawan rocks. USGS Prof. Pap. 760, 42.
Borradaile, G., Middleton, R., 2006. Proterozoic paleomagnetism in the Nipigon Embayment of northern Ontario: Pillar Lake Lava, Waweig Troctolite andGunflint Fomation tuffs. Precambr. Res. 144, 69–91.
Browning, T., Beske-Diehl, S., 1987. Paleomagnetism and the age of copper mineralization in the Portage Lake volcanics, Upper Peninsula, Michigan. Can. J. Earth Sci. 24, 2396–2404.
Chauvin, A., Perroud, H., Bazhenov, M., 1996. Anomalous low paleomagnetic inclinations from Oliogocene-Lower Miocene red beds of the south-west TienShan, Central Asia. Geophys. J. Int. 126, 303–313.
Constable, C., Johnson, C., 1999. Anisotropic paleosecular variation models: implications for geomagnetic field observables. Phys. Earth Planet. Int. 115, 35–51.
Constable, C., Parker, R.L., 1988. Statistics of the geomagnetic secular variation for the past 5 m.y. J. Geophys. Res. 93, 11569–11581.
Cox, A.V., Doell, R.R., Dalrymple, G.B., 1963. Geomagnetic polarity epochs and Pleistocene geochronometry. Nature 198, 1049–1051.
Davis, D., Paces, J., 1990. Time resolution of geologic events on the Keweenaw Peninsula and implications for development of the Midcontinent Rift system. Earth Planet. Sci. Lett. 97, 54–64.
Davis, D., Sutcliffe, R., 1985. U–Pb ages from the Nipigon plate and northern Lake Superior. Geol. Soc. Am. Bull. 96, 1572–1579.
Davis, D.W., Green, J.C., 1997. Geochronology of the North American Midcontinent rift in western Lake Superior and implications for its geodynamic evolution. Can. J. Earth Sci. 34 (4), 476–488.
Dubois, P., 1962. Paleomagnetism and correlation of Keweenawan rocks. Geol. Surv. Canada Bull. 71, 75pp.
Evans, M., 1976. Test of the dipolar nature of the geomagnetic field throughout Phanerozoic time. Nature 262, 676–677.
Fisher, R.A., 1953. Dispersion on a sphere. Proc. Roy. Soc. London, Ser. A 217, 295–305.
Green, J., Fitz, T.I., 1993. Extensive felsic lavas and rheoignimbrites in the Keweenawan Midcontinent rift plateau volcanics, Minnesota: petrographic and field recognition. J. Volc. Geotherm. Res. 54, 177–196.
Halls, H., 1974. A paleomagnetic reversal in the Osler volcanic group, Northern Lake Superior. Can. J. Earth Sci. 11, 1200–1207.
Halls, H., Palmer, H., 1981. Remagnetization in Keweenawan rocks, Part II: lava flows within the Copper Harbor Conglomerate, Michigan. Can. J. Earth Sci. 18, 1395–1408.
Halls, H., Pesonen, L., 1982. Paleomagnetism of Keweenawan rocks. Geol. Soc. Am. Mem. 156, 173–201.
Hnat, J.S., van der Pluijm, B.A., van der Voo, R., 2006. Primary curvature in the Mid-Continent Rift: paleomagnetism of the Portage Lake Volcanics (northern Michigan, USA). Tectonophysics 425 (1–4), 71–82.
Kean, W.F., Williams, I., Chan, L., Feeney, J., 1997. Magnetism of the Keweenawan age Chengwatana lava flows, northwest Wisconsin. Geophys. Res. Lett. 24 (12), 1523–1526.
Kent, D., Smethurst, M., 1998. Shallow bias of paleomagnetic inclinations in the Paleozoic and Precambrian. Earth Planet. Sci. Lett. 160, 391–402.
Kent, D.V., Tauxe, L., 2005. Corrected Late Triassic latitudes for continents adjacent to the North Atlantic. Science 307, 240–244.
King, R.F., 1955. The remanent magnetism of artificially deposited sediments. Mon. Nat. R. Astr. Soc., Geophys. Suppl. 7, 115–134.
Kirschvink, J.L., 1980. The least-squares line and plane and the analysis of paleomagnetic data. Geophys. Jour. Roy. Astron. Soc. 62, 699–718.
Krijgsman, W., Tauxe, L., 2004. Shallow bias in Mediterranean paleomagnetic directions caused by inclination error. Earth Planet. Sci. Lett. 222, 685–695.
Lawrence, K.P., Tauxe, L., Staudigel, H., Constable, C., Koppers, A., McIntosh, W.C., Johnson, C.L., 2009. Paleomagnetic field properties near the southern hemisphere tangent cylinder. Geochem. Geophys. Geosyst. 10, Q01005, doi:10.1029/2008GC00207.
Li, Z., Bogdanova, S., Collins, A., Davidson, A., DeWaele, B., Ernst, R.E., Fitzsimons, I., Fuck, R., Gladkochub, D., Jacobs, J., Karlstrom, K., Lu, S., Natapov, L., Pease, V., Pisarevsky, S., Thrane, K., Vernikovsky, V., 2008. Assembly, configuration, and break-up history of Rodinia: A synthesis. Precambr. Res. 160, 179–210.
McElhinny, M., Lock, J., 1996. IAGA paleomagnetic databases with Access. Surv. of Geophys. 17, 575–591.
McElhinny, M.W., McFadden, P.L., 1997. Palaeosecular variation over the past 5 Myr based on a new generalized database. Geophys. J. Int. 131 (2), 240–252.
McFadden, P.L., McElhinny, M.W., 1988. The combined analysis of remagnetization circles and direct observations in paleomagnetism. Earth Planet. Sci. Lett. 87, 161–172.
McFadden, P.L., McElhinny, M.W., 1990. Classification of the reversal test in palaeomagnetism. Geophys. J. Int. 103, 725–729.
Meert, J., Tamrat, E., Spearman, J., 2003. Non-dipole fields and inclination bias: insights from a random walk analysis. Earth Planet. Sci. Lett. 214, 395–408.
Merrill, R.T., McElhinny, M.W., McFadden, P.L., 1996. The Magnetic Field of the Earth: Paleomagnetism, the Core and the Deep Mantle. Academic Press.
Miller, J., Green, J., Severson, M., Chandler, V., Peterson, D., 2001. Geologic map of the Duluth Complex and related rocks, northeastern Minnesota.
Opdyke, N.D., Henry, K.W., 1969. A test of the dipole hypothesis. Earth Planet. Sci. Lett. 6, 139–151.
Paces, J., Miller, J., 1993. Precise U-Pb ages of Duluth Complex and related mafic intrusions, Northeastern Minnesota: Geochronological insights to physical petrogenetic, paleomagnetic and tectonomagmatic processes associated with the 1.1 Ga midcontinent rift system. J. Geophy. Res. 98, 13997–14013.
Palmer, H., 1970. Paleomagnetism and correlation of some Middle Keweenawan rocks, Lake Superior. Can. J. Earth Sci. 7, 1410–1436.
Palmer, H., Davis, D., 1987. Paleomagnetism and U–Pb geochronology of volcanic rocks from Michipoicoten Island, Lake Superior, Canada: precise calibration of the Keweenawan polar wander track. Precambrian Res. 37, 157–171.
Palmer, H.C., Halls, H.C., Pesonen, L.J., 1981. Remagnetization in Keweenawan rocks. Part I: conglomerates. Can. J. Earth Sci. 18, 599–618.
Pesonen, L.J., Nevanlinna, H., 1981. Late Precambrian Keweenawan asymmetric reversals. Nature 294, 436–439.
Quidelleur, X., Courtillot, V., 1996. On low-degree spherical harmonic models of paleosecular variation. Phys. Earth Planet. Int. 95, 55–77.
Robertson, W., 1973. Pole positions from the Mamainse Point lavas and their bearing on a Keweenawan pole path and polarity sequence. Can. J. Earth Sci. 10, 1541–1555.
Robertson, W., Fahrig, W., 1971. The Great Logan Paleomagnetic Loop - The polar wandering path from Canadian shield rocks during the Neohelikian Era. Can. J. Earth Sci. 8, 1355–1372.
Rochette, P., Tamrat, E., Féraud, G., Pik, R., Courtillot, V., Ketefo, E., Coulon, C., Hoffman, C., Vandamme, D., Yirgu, G., 1998. Magnetostratigraphy and timing of the Oligocene Ethiopian traps. Earth Planet. Sci. Lett. 164, 497–510.
Sandberg, A., 1938. Section across Keweenawan lavas at Duluth, MN. Geol. Soc. Am. Bull. 49, 795–830.
Schmidt, P.W., Williams, G.E., 2003. Reversal asymmetry in Mesoproterozoic overprinting of the 1.88-Ga Gunflint Formation, Ontario, Canada: non-dipole effects or apparent polar wander? Tectonophysics 377 (1–2), 7–32.
Sohl, L.E., Christie-Blick, N., Kent, D.V., 1999. Paleomagnetic polarity reversals in Marinoan (ca. 600 Ma) glacial deposits of Australia: Implications for the duration of low-latitude glaciation in neoproterozoic time. Geol. Soc. Amer. Bull. 111 (8), 1120–1139.
Tauxe, L., 2005. Inclination flattening and the geocentric axial dipole hypothesis. Earth Planet. Sci. Lett. 233, 247–261.
Tauxe, L., Banerjee, S.K., Butler, R., van der Voo, R., 2009. Essentials of Paleomagnetism. University of California Press, Berkeley.
Tauxe, L., Kent, D.V., 2004. A simplified statistical model for the geomagnetic field and the detection of shallow bias in paleomagnetic inclinations: was the ancient magnetic field dipolar? In: Channell, J.E.T.e.a. (Ed.), Timescales of the Paleomagnetic Field, vol. 145. American Geophysical Union, Washington, DC, pp. 101–116.
Tauxe, L., Kodama, K., Kent, D.V., 2008. Testing corrections for paleomagnetic inclination error in sedimentary rocks: a comparative approach. Phys. Earth Planet. Int. 169, 152–165.
Tauxe, L., Kylstra, N., Constable, C., 1991. Bootstrap statistics for paleomagnetic data. J. Geophys. Res. 96, 11723–11740.
Vandamme, D., Courtillot, V., 1992. Paleomagnetic constraints on the structure of the Deccan traps. Phys. Earth Planet. Inter. 74, 241–261.
Vervoort, J.D., Wirth, K., Kennedy, B., Sandland, T., Hatpp, K.S., 2007. The magmatic evolution of the Midcontinent rift: new geochronologic and geochemical evidence from felsic magmatism. Precambrian Res. 157 (1–4), 235–268.
Wilson, R.L., 1970. Permanent aspects of the Earth's non-dipole magnetic field over upper Tertiary times. Geophys. J. R. Astr. Soc. 19, 417–437.
Zartman, R., Nicholson, S., Cannon, W., Morey, G., 1997. U–Th–Pb zircon ages of some Keweenawan Supergroup rocks from the south shore of Lake Superior. Can. J. Earth Sci. 34, 549–561.